



ChemTech

## International Journal of ChemTech Research

CODEN (USA): IJCRGG ISSN: 0974-4290

Vol.7, No.3, pp 1148-1153, 2014-2015

ICONN 2015 [4<sup>th</sup> -6<sup>th</sup> Feb 2015]

International Conference on Nanoscience and Nanotechnology-2015  
SRM University, Chennai, India

# Optical Amplification with Surface Plasmon Resonance and Total Internal Reflection in Gold Nanostructure with BK<sub>7</sub> Parallel Slab

Nabamita Goswami<sup>1</sup>, Ardhendu Saha<sup>1\*</sup>, Arijit Ghosh<sup>1</sup>

<sup>1</sup>Department of Electrical Engineering, National Institute of Technology Agartala, Barjala, Jirania, Tripura (west), Pin:-799046, India.

**Abstract :** A Novel proposal towards the surface plasmon enhanced optical amplification is proposed, designed and simulated in Kretschmann geometry formed by a 500  $\mu\text{m}$  thick, 10 mm long and 5 mm wide BK<sub>7</sub> parallel slab and 29 nm thin gold layer ( $n=0.38+10.75i$ ) which is sandwiched between the said parallel slab and 20 nm thin GaAs layer ( $n=3.377$ ). This GaAs layer is pumped by 1319 nm higher order Gaussian beam of a Nd:YAG laser, which passes through a cylindrical lens thereby generating a high aspect ratio elliptical cross section to attain intensity dependent negative extinction coefficient on that 3 mm long strip of irradiated GaAs. The negative extinction coefficient of GaAs layer facilitates the amplification of the incident optical radiation at 1550 nm within the communication window at 26 °C temperature. Here the incident pulsed optical radiation of 5 mW is amplified to 274 MW through external pumping and surface plasmon resonance phenomenon by total internal reflection with three bounces along the length of said BK<sub>7</sub> parallel slab considering the Goos-Hänchen shift at the slab-Au layer interface and slab-air interface.

**Keywords:** Extinction Coefficient, Goos-Hänchen Shift, Kretschmann Geometry, cylindrical Lens.

## Introduction

Surface plasmon (SP) is an electromagnetic wave propagating along the interface of metal-dielectric and creation of this type of wave will only be possible when a p-polarized light of a particular wavelength with required angle of incidence is directed through an optical component and reflected from a metal film deposited on the optical component facet<sup>1</sup>. Under optimal condition, a large portion of optical energy is converted into a guided electromagnetic wave along the interface of the metal-dielectric<sup>2</sup>. This SP phenomenon was first observed by Wood<sup>3</sup>, theoretically investigated by Zenneck<sup>4</sup>, its existence was predicted by Ritchie<sup>5</sup> and experimentally demonstrated by Otto<sup>6</sup>, Kretschmann<sup>7</sup> and Raether<sup>8</sup>. In the presence of surface plasmon resonance (SPR) there will be a sharp rise in electric field of incident radiation at the interface gaining the energy from plasmon wave, which is termed as Electric Field Enhancement Effect (EFEE), where the output light intensity is several times greater than the incident light intensity<sup>9,10,11,12</sup>. In this way amplification of the incident radiation can be possible through SPR whereas the amplification with surface plasmon resonance in

semiconductor sub-wavelength waveguide devices by high current injection has already been observed by J.B.Khurgin *et.al.* in 2012<sup>13</sup>.

### Proposed Scheme

The proposed configuration in Fig. 1 is used to provide the SP enhanced optical amplification resulting from an excitation of SPR in the gold–GaAs interface by a TM-polarized incident laser radiation for a free space wavelength of 1550 nm at 26<sup>o</sup> C temperature. Here the configuration is formed by a BK<sub>7</sub> parallel slab, 29 nm thin gold (Au) layer ( $n=0.38+10.75i$ ) and 20 nm thin GaAs ( $n=3.377$ ) layer where the gold layer is sandwiched between the BK<sub>7</sub> parallel slab and GaAs layer. Here the BK<sub>7</sub> parallel slab is 10 mm long, 5 mm wide and 0.5 mm thick. This parallel slab is having refractive index ( $n$ ) 1.50066 with extinction coefficient ( $k$ ) zero for a free space wavelength of 1550 nm at 26<sup>o</sup> C temperature<sup>14,15</sup>. In Fig. 1 an external pumping by 1319 nm Nd:YAG laser transform the extinction coefficient value of GaAs layer from marginal positive to negative<sup>16,17</sup>. Using a cylindrical lens having radius 2 mm, focal length 3.9 mm, height 4 mm and length 6 mm a higher order Gaussian beam of 1319 nm is converted to a high aspect ratio elliptical cross sectional beam at its focal length<sup>18,19</sup>.

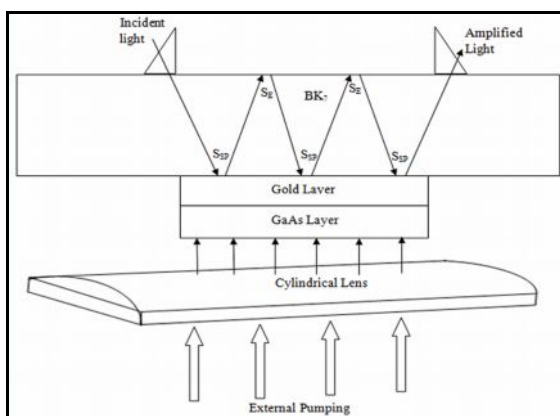


**Fig. 1: Surface plasmon enhanced optical amplifier with BK<sub>7</sub> parallel slab.**

The beam spot size through the cylindrical lens with TM<sub>00</sub> mode has been calculated by<sup>20</sup>

$$\text{Spot size} = \frac{4M^2\lambda f}{\pi D} \quad (1)$$

where  $\lambda$  is the incident wavelength,  $f$  is the lens focal length,  $D$  is the input beam diameter onto the lens and  $M^2$  is the input laser mode. In Fig. 1 the fundamental laser radiation encounters attenuated total internal reflection (ATR) at the parallel slab–gold layer interface<sup>7</sup>. ATR created evanescent wave when reaches at the gold–GaAs interface creates surface plasmon which further forms constructive interference with the evanescent wave resulting in SPR at the gold–GaAs interface<sup>1,21</sup>. In presence of the SPR wave and the external pumping wave the incident fundamental electric field experiences a sharp rise in amplitude which results in the amplification of the fundamental light intensity with the negative extinction coefficient of GaAs layer. Amplification of the incident light can be optimized for a 29 nm thin Au layer and it has been shown in Fig. 2 without considering the GaAs layer.

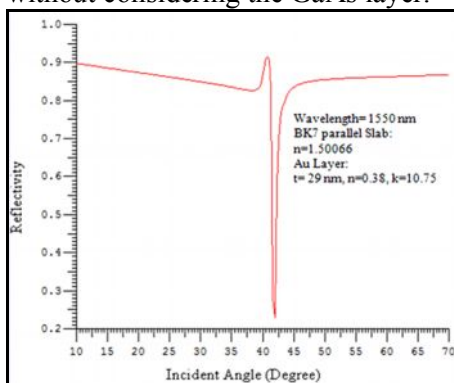


**Fig. 2: Angle of incidence vs reflectivity in absence of GaAs layer for optimizing the thickness of Au layer at 1550 nm wavelength.**

As a result, the ATR signal spectrum at 29 nm thickness of the Au layer gives a sharp plasmon dip where the reflectivity  $R$  is 0 at an incident angle of  $42.01^\circ$ . Therefore the thickness of the Au layer is optimized at 29 nm where the excited SPR photon is maximum. Now for determining the thickness of the dielectric layer for which we need to consider the presence of GaAs layer in a non-excited state, having  $n = 3.377 + 0.00013i$  at  $26^\circ\text{C}$  temperature<sup>16</sup>. The simulated maximum SPR signal spectrum is obtained at 20 nm thickness of GaAs layer with an incident angle of  $42.01^\circ$ . This 20 nm thin GaAs layer offers a low absorption loss with the extinction coefficient of 0.00013. The amplification of the incident optical radiation will only be possible if this extinction coefficient of the GaAs layer becomes negative under the influence of external pumping<sup>22, 23</sup>. This can be mathematically expressed through the following formulae<sup>24</sup>.

$$I_{out} = I_{in} \exp(-\alpha d) \quad (4)$$

$$\alpha = \frac{4\pi f' k'}{c} \quad (5)$$

$$\alpha(E) = \alpha_0 \sqrt{\frac{E - E_g}{E_g}} \quad (6)$$

where  $I_{out}$  is the output light intensity,  $I_{in}$  input fundamental light intensity,  $\alpha$  is the absorption coefficient,  $d$  is the path length,  $f'$  is the frequency of the incident light,  $k'$  is the extinction coefficient of the material,  $c$  is the velocity of light in free space,  $\alpha(E)$  is the absorption coefficient as a function of  $E$ ,  $\alpha_0$  is a constant having different numerical values for different materials,  $E$  is the amount of energy higher than the band gap energy,  $E_g$  is the band gap energy. The above equation clearly indicates that 20 nm thin GaAs layer for a pump power level of 3.1043 mW at a wavelength of 1319 nm steered through the cylindrical lens transforms the extinction coefficient of GaAs layer from marginal positive to negative. This optical pumping by pump laser creates a population inversion in the GaAs dielectric layer, which delivers adequate energy to excite the plasmon field further<sup>22, 23</sup>. Here the pump source is a 1319 nm CW micro chip DPSS Nd:YAG laser,  $E_g = 1.42$  eV and  $\alpha_0 = 2.3 \times 10^4/\text{cm}$  for 20 nm thin GaAs layer, which turns the extinction coefficient of GaAs layer from 0.00013 to -0.755534. The variation of amplified output with the variation of incident angle from this SPR configuration formed by BK<sub>7</sub> parallel slab coated with Au layer and optically pumped GaAs layer having negative extinction coefficient is shown in Fig. 3.

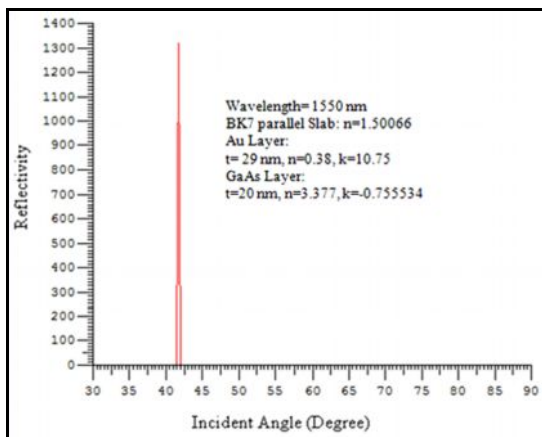


**Fig. 3: Angle of incidence vs reflectivity with –ve extinction coefficient of GaAs layer and optimum hicknesses of different layers at  $26^\circ\text{C}$  temperature.**

The peak reflectivity of the order of  $10^3$  is found at  $41.83^\circ$  angle of incidence for a single bounce.

For multiple bounce at an incident angle greater than the critical angle within BK<sub>7</sub> parallel slab the phase shifts of the incident radiation contributed by Goos-Hänchen (GH) shift with SP and without SP need to be considered. In the bottom portion of the parallel slab the GH shift with SP can be expressed through<sup>25</sup>

$$S_{sp} = -\frac{1}{k} \frac{d\phi}{d\theta} \quad (7)$$

$$k = \frac{2\pi}{\lambda} \quad (8)$$

where  $\phi$  is the phase difference between the incident light beam and reflected light beam,  $\theta$  is the angle of incidence and  $k$  is the wave vector in the medium of incidence<sup>26</sup>. Here

$$\phi = \tan^{-1} \frac{\text{Im}(N \times D^*)}{\text{Re}(N \times D^*)} \quad (9)$$

where  $N$  and  $D$  represent the numerator and denominator of the reflection coefficient of three layer structure ( $r_{123}$ ) and this can be defined by<sup>27</sup>

$$r_{123} = \frac{r_{12} + r_{23} \exp(2ik_{z2}d_2)}{1 + r_{12}r_{23} \exp(2ik_{z2}d_2)} \quad (10)$$

where  $r_{ij}$  is the Fresnel reflection coefficient,  $k_{iz}$  is the normal component of wave vectors in each medium,  $d_2$  is the metal thickness respectively. For single bounce the change in phase difference  $\phi$  with the variation of incident angle with a 20 nm thin Au layer and 29 nm thin GaAs layer is shown in Fig. 4.

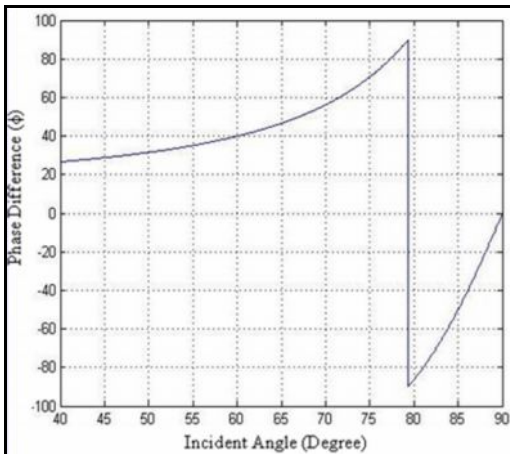


**Fig. 4: Angle of incidence vs Phase difference ( $\phi$ ) for single bounce.**

The GH shift,  $S_{sp}$  given in Equ<sup>n</sup> (7) due to SP ( $S_{sp}$ ) is -89.055 nm at the earlier optimized incident angle of 41.83<sup>o</sup>. Now in our proposed configuration the GH shift without SP for single bounce can be defined by<sup>28</sup>

$$S_E = \left(\frac{2}{k_1}\right) \frac{\tan \alpha_c}{\sqrt{\sin^2 \theta - \sin^2 \alpha_c}} \quad (11)$$

where  $\theta$  is the incident angle,  $\alpha_c$  is the critical angle and  $k_1$  is the propagation constant in the medium. As total internal reflection has been encountered for every bounce, therefore the GH shift without SP at an incident angle of 41.83<sup>o</sup> will be 14.755  $\mu\text{m}$ . The surface roughness owing to fabrication defect of the parallel slab of BK<sub>7</sub> needs to be considered. The reflectivity due to surface roughness for single bounce is given by<sup>29,30</sup>

$$R = \exp[-((4\pi n_j \sigma \cos \theta) / \lambda)^2] \approx 1 - ((4\pi n_j \sigma \cos \theta) / \lambda)^2 \quad (12)$$

where  $n_j$  is the refractive index of the medium,  $\sigma$  is the surface roughness standard deviation (p-v value/12) and  $j=1$ . In Fig.1 the calculated reflectivity due to surface roughness is 0.99977 after considering the p-v value of 31.85 nm<sup>31</sup>.

## Conclusion

A new approach of surface plasmon enhanced optical amplification at a wavelength of 1550 nm by total internal reflection in a 10 mm long BK<sub>7</sub> parallel slab within the effective length of 3 mm resulting 3 bounces for an incidence angle of 41.83° has been explored here analytically. Simulated data clearly indicates the amplification of optical radiation having peak power of 5 mW to 274 MW. GH shift observed in the surface plasmon interaction point as -89.055 nm and GH shift observed in parallel slab-air boundary is 14.755 μm for each bounce. Surface roughness of the parallel slab at slab air interface has also been considered for the proposed configuration. This concept of amplification can be futuristic tool for surface plasmon enhanced multimode waveguide based devices.

## References

1. Raether, H., Surface plasmons on smooth and rough surfaces and on gratings, Volume 111, Springer-Verlag, 1988.
2. Huang, Y., Ho, H.P., Kong, S.K. and Kabashin, A.V., Phase-sensitive surface plasmon resonance biosensors: methodology, instrumentation and applications, *Annalen Der Physik (Berlin)* 2012, 524, 637-662.
3. Wood, R.W., On a remarkable case of uneven distribution of light in a diffraction grating spectrum, *Philosophical Magazine* 1902,4, 396-402.
4. Zenneck, J., Über die Fortpflanzung ebener elektromagnetischer Wellen längs einer ebenen Leiterfläche und ihre Beziehung zur drahtlosen Telegraphie, *Annalen der Physik (Berlin)* 328, 1907, 846-866.
5. Ritchie, R.H., Plasma losses by fast electrons in thin films, *Physical Review* 106 (1957) 874-881.
6. Otto, A.Z., Excitation of nonradiative surface plasma waves in silver by the method of frustrated total reflection, *Zeitschrift fur Physik*, 1968, 216, 398-410.
7. Kretschmann, E., The determination of the Optical Constants of Metals by Excitation of Surface Plasmons, *Zeitschrift fur Physik*, 1971, 241, 313-324.
8. Kretschmann, E. and Raether, H., Radiative decay of non radiative surface plasmons excited by light, *Z. Phys.* 1968, 239, 2135-2136.
9. Takano, T., Okada, Y., Inoue, Y., Yano, K. and Tokumaru, T., Optical Harmonic Generator, United States Patent, 5,073,725, 1991.
10. Hu, J., Li, W.D., Ding, F. and Chou, S.Y., Effects of nanodots on surface plasmons and electric field enhancement in nano-pillar antenna array, *Proceedings of Lasers and Electro-Optics (CLEO) and Quantum Electronics and Laser Science Conference (QELS)*, 978-1-55752-889-6, 2010, 16.
11. Saha, A. and Goswami, N., Long range surface plasmon enhanced reflected second harmonic and fourth harmonic generation in the same fused silica prism, *Optics Communications* 2013,297, 109-112.
12. Grubisic, A., Ringe, E., Cobley, C.M., Xia, Y., Marks, L.D., Van Duyne, R.P. and Nesbitt, D.J., Plasmonic near-electric field enhancement effects in ultrafast photoelectron emission: correlated spatial and laser polarization microscopy studies of individual Ag nanocubes, *Nano Letters*, 2012,12, 4823-4829.
13. Sun, G. and Khurgin, J.B., Practicality of compensating the loss in the plasmonic waveguides using semiconductor gain medium, *Applied Physics Letters*, 2012,100, 011105-3.
14. Schulz, L.G., The optical constants of silver, gold, copper and aluminum: I. The absorption coefficient k, *Journal of the Optical Society of America*, 1954, 44, 357-362.
15. Ordal, M.A., Long, L.L., Bell, R.J., Bell, S.E., Alexander, R.W. and Ward, C.A., Optical properties of the metals Al, Co, Cu, Au, Fe, Pb, Ni, Pd, Pt, Ag, Ti, and W in the infrared and far infrared, *Applied Optics* 1983,22, 1099-1020.
16. Matsumoto, T., Optical Amplifier Using Photoelectric Effect Of Surface Plasmon Resonance Photons And Its Manufacturing Method, United States Patent, US 2009/0296200 A1, 2009.
17. Madelung, O., Rossler, U. and Schulz, M., Germanium (Ge) solubility and segregation data of impurities: groups I–VIII, Springer Berlin Heidelberg, 2002.

18. Jacobs, D.H., Fundamentals of Optical Engineering, First ed., McGraw-Hill Book Co., 1943.
19. [http://www.thorlabs.com/newgrouppage9.cfm?objectgroup\\_id=2803](http://www.thorlabs.com/newgrouppage9.cfm?objectgroup_id=2803)
20. [http://www.iivinfrared.com/resources/spot\\_size.html](http://www.iivinfrared.com/resources/spot_size.html) .
21. Tang, Y., Zeng, X. and Liang, J., Surface Plasmon Resonance: An Introduction to a Surface Spectroscopy Technique, Journal of Chemical Education 2010, 87, 742-746.
22. Seidel, J., Grafstrom, S. and Eng, L.M., Stimulated emission of surface plasmons at the interface between a silver film and an optically pumped dye solution, Physical Review Letters, 2005, 94, 177401.
23. Noginov, M.A., Podolskiy, V.A., Zhu, G., Mayy, M., Bahoura, M., Adegoke, J.A., Ritzo, B.A. and Reynolds, K., Compensation of loss in propagating surface plasmon polariton by gain in adjacent dielectric medium, Optics express, 2008,16, 1385-1392.
24. Beer, Bestimmung der Absorption des rothen Lichts in farbigen Flüssigkeiten, Annalen der Physik und Chemie, 1852, 86, 78-88.
25. Artmann, K., Calculation of the Lateral Shift of Totally Reflected Beams, Annalen der Physik (Leipzig), 1948, 2, 87-86.
26. Sasagawa, K. and Tsuchiya, M., Highly efficient third harmonic generation in a periodically poled MgO, Applied Physics Express, 2009, 2, 122401.
27. Yang, X., Liu, D. and Xie, W., High-sensitivity Optical Sensor Based on Surface Plasmon Resonance Enhanced Goos-Hanchen shift, Proceedings of IEEE 9808482, 2006, 74-77.
28. Snyder, A.W. and Love, J.D., Goos-Hanchen shift, Applied Optics, 1976,15, 236-238.
29. Baudrier-Raybaut, M., Haidar, R., Kupecek, P., Lemasson, P., Rosencher, E., Random quasi-phase-matching in bulk polycrystalline isotropic nonlinear materials, Nature 2004,432, 374-376.
30. Saha, A. and Deb, S., Broadband second harmonic generation in a tapered isotropic semiconductor slab using total internal reflection quasi phase matching, Optics Communication, 2011, 284; 4714-4722.
31. [http://www.laser2000.co.uk/optics\\_&\\_optomechanics.php?Category=164](http://www.laser2000.co.uk/optics_&_optomechanics.php?Category=164).

\*\*\*\*\*